Simple Solution to Optimal Cotangential Transfer between Coplanar Elliptic Orbits

Alessandro A. Quarta*, Giovanni Mengali

Dipartimento di Ingegneria Civile e Industriale, University of Pisa, Italy

Department of Civil and Industrial Engineering, University of Pisa, I-56122, Italy

Abstract

The aim of this paper is to propose a semi-analytical method for the analysis of a two-impulse transfer between two coplanar elliptic orbits, assuming each maneuver to change the magnitude of the spacecraft velocity only, without affecting its direction. Using a recent mathematical model that describes the spacecraft dynamics in a compact analytical form within a two-dimensional multiple-impulse scenario, this work proposes an algorithm to calculate the global minimum velocity variation required to complete the transfer. The characteristics of the optimal transfer trajectory, which is tangent to both the parking and the target orbit, are obtained as a function of a single variable, which defines the angular position of the first maneuver. This feature allows the designer to analyze the cotangential transfer in a parametric form, thus obtaining a trade-off solution between the total velocity variation and the desired characteristics of the transfer orbit.

Keywords: Two-impulse transfer, Tangential impulsive maneuvers, Mission design

Nomenclature

a, b	=	auxiliary dimensionless functions, see Eqs. (33)-(34)
D, N	=	auxiliary dimensionless functions, see Eqs. (7)-(8)
e	=	orbital eccentricity
f, g, G	=	auxiliary dimensionless functions, see Eqs. (30)-(31) and (39)
H	=	Heaviside step function
J	=	performance index
n	=	number of impulsive maneuvers
O	=	primary body center-of-mass
p	=	semilatus rectum
r	=	primary body-spacecraft distance
ΔV	=	velocity variation
$\Delta\theta$	=	swept angle
η	=	dimensionless parameter, see Eq. (4)
θ	=	polar angle
μ	=	primary body gravitational parameter
ψ	=	auxiliary angle, see Eq. (36)
ω	=	apse line rotation angle

*Corresponding author

Email addresses: a.quarta@ing.unipi.it (Alessandro A. Quarta), g.mengali@ing.unipi.it (Giovanni Mengali)

Published in Acta Astronautica, Vol. 155 February 2019, pp. 247–254. doi: http://dx.doi.org/10.1016/j.actaastro.2018.12.007

Subscripts

0	=	parking orbit
1	=	transfer trajectory, first maneuver
2	=	target orbit, second maneuver
i	=	i-th maneuver, Keplerian arc

Superscripts

$\star$	=	optimal

1. Introduction

A fundamental requirement for the success of most space missions is the capability for a spacecraft to achieve and maintain a predetermined orbit. For example, it is often required to correct the shape, size, and/or orientation of an intermediate or parking orbit by means of propulsive maneuvers since the launch vehicle usually cannot deploy the satellite in its final, working, orbit. Other typical applications include trajectory or midcourse maneuvers, change of the orbital inclination and rendezvous guidance problems [1]. A particularly complex scenario is represented by the reconfiguration maneuver of several spacecraft that operate in a formation. In most cases the problem may be reduced to look for impulsive maneuvers that are able to transfer a spacecraft from a given elliptic orbit to another prescribed elliptic orbit. A very readable and thorough introduction to this subject is offered by the classical survey paper by Gobetz and Doll [2].

In this context, this paper concentrates on finding a transfer Keplerian trajectory that is tangent to two coplanar ellipses (often referred to as cotangential transfer). The latter may be considered a classical problem of orbital mechanics, which was first investigated by Lawden [3] in a two-impulse mission scenario. Early attempts to find a solution to the cotangential transfer were based on graphical methods, which exploited the hodograph theory [4]. In particular, Thompson et al. [5] used the orbital hodograph theory to deal with the cotangential transfer within the context of safety improvements of orbital rendezvous. The rationale is that, in case the rendezvous maneuver is eventually aborted [6], a transfer tangent to the final trajectory allows the spacecraft to smoothly move away from the target orbit without crossing it. The solution presented in Ref. [5] is based on a numerical iterative procedure to find the cotangential orbit. More recently, Zhang et al. [7, 8] analyzed the constrained reachable domain [9, 10, 11] with a single tangential impulse, and proposed an analytical approach for the study of the conditions under which a cotangential transfer exists, in terms of true anomaly range along the initial or final orbit. Indeed, a cotangential transfer may not be feasible when the two terminals belong to intersecting elliptic orbits [12]. The importance of a cotangential transfer has been recently stressed by Kiriliuk and Zaborsk [13], who have analyzed the optimal bi-elliptic (and bi-parabolic) transfer trajectories between non-coaxial elliptic orbits. Finally, the future research should try to extend this problem to general relativistic fields either to devise some possible tests or to account for it in some special cases when extreme accuracy may be needed [14, 15].

Since for a given pair of arbitrarily oriented coplanar elliptic orbits there exists an infinite number of admissible cotangential transfer ellipses [16], a particularly interesting problem is to look for the optimal impulsive trajectory [17], that is, the transfer that minimizes the total velocity variation (ΔV). A solution to this problem cannot be obtained in closed-form, and it has been pointed out that in some cases the total ΔV tends to be sensitive to the initial position point, especially when the two reference orbits have intersection points [2]. Vinh [18] has shown that, in general, a cotangential transfer is not optimal when a truly minimum ΔV transfer trajectory is sought. However, when the two reference elliptic orbits are of low eccentricity, that is, less than 0.2, a cotangential transfer is known to be near optimal. In fact, in that case the total velocity variation exceeds the global minimum value (which would correspond to a non-tangent transfer) by less than 1% only [19].

The aim of this paper is to illustrate an effective procedure for calculating the optimal two-impulse cotangential transfer between two coplanar elliptic orbits. The proposed method is different from other existing approaches [20] and is especially well suited for obtaining a simple expression for the required ΔV. It exploits a recent mathematical model that describes, in a compact analytical form, the spacecraft two-dimensional dynamics within a generic multiple-impulse scenario [21]. The characteristics of the transfer

trajectory are obtained as a function of a single independent variable that defines the angular position of the first impulsive maneuver along the parking orbit. The described method allows the designer to analyze the cotangential transfer in a parametric form and, using a graphical approach, to easily select the best trade-off solution between the (two-impulse) total ΔV and the desired characteristics of the transfer orbit.

2. Problem description and mathematical model

Consider two elliptic, coplanar and confocal Keplerian orbits of given shape and orientation. The common focus of the two orbits is denoted by O and μ is the gravitational parameter of the primary body. Let $e_0 < 1$ and p_0 be the eccentricity and semilatus rectum of the parking orbit, respectively, and introduce the subscript 2 for indicating the orbital parameters of the target orbit, whose apse line (from the focus to the pericenter) is rotated counterclockwise by an angle $\omega_2 \in [0,\, 2\,\pi)$ with respect to that of the parking orbit, see Fig. 1.

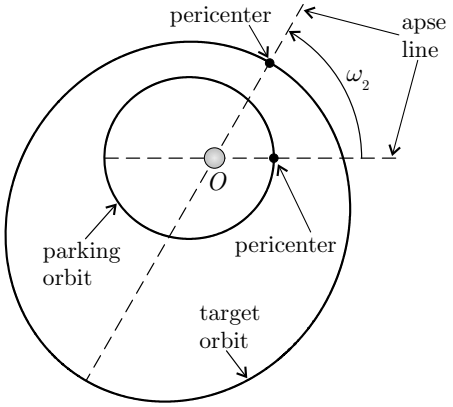

Figure 1: Problem geometry.

The problem addressed in this work is to find the optimal trajectory (subscript 1), in terms of minimum required ΔV, which allows the spacecraft to be transferred from the parking to the target orbit by means of two tangential impulsive maneuvers (TIMs). By definition, the two maneuvers may only change the magnitude of the spacecraft velocity vector without affecting its direction. In other terms, if ΔV_1 (or ΔV_2) is the velocity variation relative to the first (or the second) TIM, the characteristics of the cotangent transfer orbit, that is, its semilatus rectum p_1, eccentricity e_1 and apse line rotation angle $\omega_1 \in [0,\, 2\,\pi)$ relative to the parking orbit apse line, have to be chosen such that the dimensionless performance index

$$J \triangleq \frac{\Delta V}{\sqrt{\mu/p_0}} = \frac{\Delta V_1 + \Delta V_2}{\sqrt{\mu/p_0}} \tag{1}$$

is minimized. Note that $\sqrt{\mu/p_0}$ is a reference velocity that coincides with the orbital velocity of a (virtual) circular orbit of radius p_0, around the primary body O.

The study of this problem, which requires the use of two TIMs, may be thought of as a special case of a transfer orbit in which the spacecraft performs a sequence of $n \in \mathbb{N}^+$ TIMs, with $n = 2$. It is therefore possible to analyze the transfer trajectory by exploiting the general mathematical model discussed in Ref. [21], which uses a linear systems approach to study the two-dimensional spacecraft motion in a multiple-impulse (either radial or tangential) mission scenario. The main features of such a model, which are useful for the succeeding analysis, are now briefly summarized.

2.1. Mathematical preliminaries

Consider a spacecraft, initially placed on an elliptic parking orbit with orbital parameters $\{p_0,\, e_0\}$, which executes $n \geq 1$ TIMs. Assuming the spacecraft to be under the gravitational attraction of the primary only, its trajectory belongs, at any time, to the same plane as that of the parking orbit and consists of $(n+1)$ conic arcs, each one being characterized by a semilatus rectum p_i, an eccentricity e_i, and an apse line rotation

angle $\omega_i \in [0,\, 2\,\pi)$, with $i = 1, 2, \ldots, n$. Note that ω_i is measured counterclockwise from the parking orbit apse line. The three parameters $\{p_i, e_i, \omega_i\}$ univocally define the geometry of the i-th conic arc that starts just after the application of the i-th TIM. The index $i = 0$ corresponds to the given parking orbit, while $i = n$ (just after the last maneuver) represents the target Keplerian orbit, see Fig. 2.

According to Ref. [21], the polar equation of the spacecraft trajectory can be written in a compact and analytical form as

$$r = r(\theta) = \frac{p_0}{1 + e_0\, \cos\theta + \displaystyle\sum_{i=1}^{n} \frac{1-\eta_i^2}{\prod_{j=1}^{i} \eta_j^2}\, \left[1 - \cos(\theta - \theta_i)\right]\, H(\theta - \theta_i)} \tag{2}$$

where r is the primary-spacecraft distance, $\theta \geq 0$ is the polar angle measured counterclockwise from the parking orbit apse line, and $H(x)$ denotes the Heaviside step function, defined as

$$H(x) = \begin{cases} 0 & \text{if} \quad x \leq 0 \\ 1 & \text{if} \quad x > 0 \end{cases} \tag{3}$$

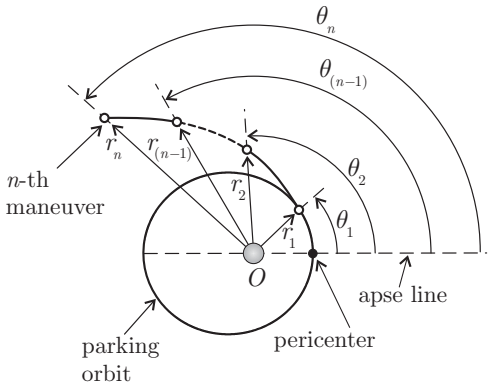

Figure 2: Multiple impulse transfer conceptual sketch.

In Eq. (2), $\theta_i \geq 0$ is the polar angle at which the i-th TIM is executed, while $\eta_i > 0$ is a dimensionless and strictly positive parameter defined as

$$\eta_i \triangleq \sqrt{\frac{p_i}{p_{(i-1)}}} \tag{4}$$

where $p_{(i-1)}$ is the semilatus rectum of the Keplerian orbit just before the i-th TIM. The values of e_i and ω_i are obtained from equations

$$e_i = \prod_{j=1}^{i} \eta_j^2 \sqrt{N_i^2 + D_i^2} \tag{5}$$

$$\sin\omega_i = -\frac{N_i}{\sqrt{D_i^2 + N_i^2}} \quad , \quad \cos\omega_i = \frac{D_i}{\sqrt{D_i^2 + N_i^2}} \tag{6}$$

where the dimensionless functions N_i and D_i are defined as

$$N_i \triangleq \sum_{k=1}^{i} \frac{1-\eta_k^2}{\prod_{j=1}^{k} \eta_j^2}\, \sin\theta_k \tag{7}$$

$$D_i \triangleq e_0 - \sum_{k=1}^{i} \frac{1-\eta_k^2}{\prod_{j=1}^{k} \eta_j^2}\, \cos\theta_k \tag{8}$$

Note, in passing, that Eq. (6) fixes a typo (that is, a minus sign) in Eq. (36) of Ref. [21]. Finally, the velocity variation ΔV_i of the i-th TIM may be written in a compact form as

$$\Delta V_i = |\eta_i - 1| \sqrt{\frac{2\,\mu}{r_i} - \frac{\mu\,\left(1 - e_{i-1}^2\right)}{p_{i-1}}} \tag{9}$$

where r_i is the primary-spacecraft distance at which the i-th TIM is executed, see Eq. (2). The total velocity variation ΔV is therefore

$$\Delta V = \sum_{i=1}^{n} \Delta V_i \tag{10}$$

The previous relations may be applied to a generic number $n \in \mathbb{N}^+$ of TIMs. In particular, for a given set of n polar angles $\{\theta_1, \theta_2, \ldots, \theta_n\}$, the whole spacecraft trajectory is defined by Eq. (2), the characteristics of each Keplerian arc (semilatus rectum, eccentricity and apse line direction) are obtained from Eqs. (4)–(6), each velocity variation is given by Eq. (9), and the total ΔV is calculated through Eq. (10).

2.2. Case of two-TIM transfer

In the notable case of a two-impulse transfer ($n = 2$), the previous relations may be used to define an algorithm for finding the absolute minimum of the performance index J in Eq. (1) using a graphical approach. To that end, note that the first maneuver point, which belongs to the parking orbit, has a polar angle $\theta_1 \in [0,\, 2\,\pi)$ that coincides with its true anomaly. Also, since the second maneuver point belongs to the target orbit, its polar angle $\theta_2 > \theta_1$ may be written as

$$\theta_2 = \theta_1 + \Delta\theta \qquad \text{with} \qquad \Delta\theta \in (0,\, 2\,\pi) \tag{11}$$

In fact, if $\Delta\theta > 2\pi$, the spacecraft would travel more than one full revolution along the transfer orbit when $e_1 < 1$. Using Eq. (11), $\Delta\theta$ may therefore be used as the angular variable necessary to set the second maneuver point, with $\Delta\theta \neq 0$.

The characteristics of the transfer orbit are obtained from Eqs. (4)–(6) by simply enforcing the condition $i = 1$, viz.

$$p_1 = p_0\,\eta_1^2 \tag{12}$$

$$e_1 = \eta_1^2 \sqrt{e_0^2 - 2\,e_0\,\left(1/\eta_1^2 - 1\right)\,\cos\theta_1 + \left(1/\eta_1^2 - 1\right)^2} \tag{13}$$

$$\sin\omega_1 = -\frac{N_1}{\sqrt{N_1^2 + D_1^2}} \quad , \quad \cos\omega_1 = \frac{D_1}{\sqrt{N_1^2 + D_1^2}} \tag{14}$$

where the dimensionless functions N_1 and D_1 are, see Eqs. (7)-(8)

$$N_1 = \left(\frac{1}{\eta_1^2} - 1\right)\sin\theta_1 \qquad , \qquad D_1 = e_0 - \left(\frac{1}{\eta_1^2} - 1\right)\cos\theta_1 \tag{15}$$

with

$$N_1^2 + D_1^2 = e_0^2 - 2\,e_0\,\left(1/\eta_1^2 - 1\right)\,\cos\theta_1 + \left(1/\eta_1^2 - 1\right)^2 \tag{16}$$

When the condition $n = 1$ or $n = 2$ is enforced in Eq. (2), the primary-spacecraft distance is found at the first (r_1) or second (r_2) TIM as

$$r_1 = \frac{p_0}{1 + e_0\,\cos\theta_1} \tag{17}$$

$$r_2 = \frac{p_0}{1 + e_0\,\cos\theta_2 + \left(1/\eta_1^2 - 1\right)\,\left[1 - \cos(\theta_2 - \theta_1)\right]} \tag{18}$$

From Eq. (9), the velocity variations at the two maneuver points are

$$\Delta V_1 = |\eta_1 - 1| \sqrt{\frac{2\,\mu}{r_1} - \frac{\mu\ (1 - e_0^2)}{p_0}} \tag{19}$$

$$\Delta V_2 = |\eta_2 - 1| \sqrt{\frac{2\,\mu}{r_2} - \frac{\mu\ (1 - e_1^2)}{p_1}} \tag{20}$$

Substituting Eqs. (17)-(18) into (19)-(20), it may be verified that

$$\Delta V_1 = \sqrt{\frac{\mu_\odot}{p_0}}\, |\eta_1 - 1| \sqrt{e_0^2 + 2\, e_0\ \cos\theta_1 + 1} \tag{21}$$

$$\Delta V_2 = \sqrt{\frac{\mu_\odot}{p_0}}\, |\eta_2 - 1| \sqrt{\eta_1^2\, [e_0^2 + 2\, e_0\ \cos\theta_1 + 1] + 2\, e_0\ (\cos\theta_2 - \cos\theta_1) + 2\ (1/\eta_1^2 - 1)\ [1 - \cos\left(\theta_2 - \theta_1\right)]} \tag{22}$$

and the dimensionless performance index of Eq. (1) can be explicitly written as

$$J = J\left(\eta_1, \eta_2, \theta_1, \theta_2\right) = |\eta_1 - 1| \sqrt{e_0^2 + 2\, e_0\ \cos\theta_1 + 1} + \\ + |\eta_2 - 1| \sqrt{\eta_1^2\, [e_0^2 + 2\, e_0\ \cos\theta_1 + 1] + 2\, e_0\ (\cos\theta_2 - \cos\theta_1) + 2\ (1/\eta_1^2 - 1)\ [1 - \cos\left(\theta_2 - \theta_1\right)]} \tag{23}$$

However, the four mission parameters $\{\eta_1,\, \eta_2,\, \theta_1,\, \theta_2\}$ in the performance index J are not independent. Indeed, at the end of the second maneuver the spacecraft belongs to the target orbit, whose orbital parameters $\{p_2,\, e_2,\, \omega_2\}$ are given. Substituting $i = 2$ into Eqs. (4)–(6), the result is

$$p_2 = p_0\, \eta_1^2\, \eta_2^2 \tag{24}$$

$$e_2 = \eta_1^2\, \eta_2^2 \sqrt{\left[e_0 + \frac{(\eta_1^2 - 1)\cos\theta_1}{\eta_1^2} + \frac{(\eta_2^2 - 1)\cos\theta_2}{\eta_1^2\, \eta_2^2}\right]^2 + \left[\frac{(\eta_1^2 - 1)\sin\theta_1}{\eta_1^2} + \frac{(\eta_2^2 - 1)\sin\theta_2}{\eta_1^2\, \eta_2^2}\right]^2} \tag{25}$$

$$\tan\omega_2 = \frac{\eta_2^2\, (\eta_1^2 - 1)\sin\theta_1 + (\eta_2^2 - 1)\sin\theta_2}{\eta_1^2\, \eta_2^2\, e_0 + \eta_2^2\, (\eta_1^2 - 1)\cos\theta_1 + (\eta_2^2 - 1)\cos\theta_2} \tag{26}$$

which give three additional nonlinear constraints to be met. In conclusion, a single variable only may be freely chosen within the set $\{\eta_1,\, \eta_2,\, \theta_1,\, \theta_2\}$ and this is selected to coincide with the polar angle $\theta_1 \in [0,\, 2\,\pi)$.

Recalling Eq. (11), the previous Eqs. (24)–(26) may be rearranged in the form

$$\eta_1 = \sqrt{f(\theta_1, \Delta\theta)} \tag{27}$$

$$\eta_2 = \frac{\sqrt{p_2/p_0}}{\sqrt{f(\theta_1, \Delta\theta)}} \tag{28}$$

$$e_2 = g(\theta_1, \Delta\theta) \tag{29}$$

where $f(\theta_1, \Delta\theta)$ and $g(\theta_1, \Delta\theta)$ are two dimensionless auxiliary functions defined as

$$f(\theta_1, \Delta\theta) \triangleq \frac{(p_2/p_0)\ [\sin(\omega_2 - \theta_1) - \sin(\omega_2 - \theta_1 - \Delta\theta)]}{(p_2/p_0)\ [\sin(\omega_2 - \theta_1) + e_0\ \sin\omega_2] - \sin(\omega_2 - \theta_1 - \Delta\theta)} \tag{30}$$

$$g(\theta_1, \Delta\theta) \triangleq \frac{\sin(\Delta\theta) + (p_2/p_0)\ [e_0\ \sin\theta_1 - e_0\ \sin(\theta_1 + \Delta\theta) - \sin(\Delta\theta)]}{\sin(\omega_2 - \theta_1 - \Delta\theta) - \sin(\omega_2 - \theta_1)} \tag{31}$$

Note that $\eta_1 \neq 0 \Rightarrow p_1 \neq 0$, see Eq. (4), and so $f(\theta_1, \Delta\theta) \neq 0$, see Eq. (30), which implies that the denominator of Eq. (31) is different from zero. Combining Eqs. (29) and (31) it is found that

$$a \sin\Delta\theta + b \cos\Delta\theta - a = 0 \tag{32}$$

where

$$a \triangleq -e_0 \, (p_2/p_0) \, \sin\theta_1 - e_2 \, \sin\left(\omega_2 - \theta_1\right) \tag{33}$$

$$b \triangleq 1 - (p_2/p_0) - e_0 \, (p_2/p_0) \, \cos\theta_1 + e_2 \, \cos\left(\omega_2 - \theta_1\right) \tag{34}$$

Since $\Delta\theta \neq 0$, Eq. (32) can be rewritten as

$$\sin\left(\Delta\theta + \psi\right) - \sin\psi = 0 \tag{35}$$

where the auxiliary angle ψ is defined by

$$\sin\psi = \frac{a}{\sqrt{a^2 + b^2}} \qquad , \qquad \cos\psi = \frac{b}{\sqrt{a^2 + b^2}} \tag{36}$$

The value of $\Delta\theta \in (0,\, 2\pi)$ that satisfies Eq. (29) is given by

$$\Delta\theta = \pi - 2\,\psi \tag{37}$$

where ψ is obtained from Eqs. (33)-(34) and (36) as a function of θ_1, p_2/p_0, e_0, e_2, and ω_2. In particular, note that J in Eq. (23) depends on the semilatus rectum of the parking and target orbits as a function of their ratio p_2/p_0 only.

2.3. Algorithm for the analysis of global optimal transfer

It is now possible to describe an algorithm that minimizes the ΔV necessary for a two-impulse cotangential transfer between a given pair of elliptic orbits. Assume the characteristics of the parking and target orbits are fixed through the four parameters $\{p_2/p_0, e_0, e_2, \omega_2\}$. For a given coordinate $\theta_1 \in [0,\, 2\pi)$, $\Delta\theta$ is obtained from Eq. (37) and $f(\theta_1, \Delta\theta)$ from Eq. (30) (the case $f(\theta_1, \Delta\theta) < 0$ is discarded as it corresponds to an infeasible transfer). The values of θ_2, η_1 and η_2 are calculated from Eqs. (11), (27) and (28), respectively. Finally, J is obtained from Eq. (23). The same procedure is then repeated for different values of θ_1, until a smooth function plot $J = J(\theta_1)$ is obtained in the interval $[0,\, 2\pi)$. The optimal transfer corresponds to the polar angle $\theta_1 = \theta_1^\star \in [0,\, 2\pi)$ that minimizes $J(\theta_1)$, viz.

$$\theta_1^\star = \min_{\theta_1 \in [0,\, 2\pi)} \left[J(\theta_1)\right] \tag{38}$$

whose value can be obtained, by inspection, from the plot of $J = J(\theta_1)$.

3. Method validation and case study

The previously described algorithm is now validated by analyzing the transfer between elliptic, coplanar, orbits whose axes are aligned and have the same direction (that is, $\omega_2 = 0\,\text{deg}$). For exemplary purposes, assume $p_2/p_0 = 2$, $e_0 = 0.2$, and $e_2 = 0.4$. In this case the plot of $J = J(\theta_1)$ (that, is the total velocity variation $\Delta V/\sqrt{\mu/p_0}$ as a function of the polar angle θ_1) obtained through the proposed algorithm is shown in Fig. 3(a), while Fig. 3(b) illustrates the (dimensionless) value of $\Delta V_1 = \Delta V_1(\theta_1)$ and $\Delta V_2 = \Delta V_2(\theta_1)$.

In particular, Fig. 3(a) shows that the minimum value of J, that is, the optimal transfer in terms of minimum required ΔV, is obtained when $\theta_1 = 0$, that is, when the first maneuver occurs at the pericenter of the parking orbit. In that case, Eq. (33) gives $a = 0$, Eq. (36) gives $\psi = 0$, and Eq. (37) states that $\Delta\theta = 180\,\text{deg}$. In other terms, the optimal transfer trajectory coincides with a semi-ellipse (in fact, the swept angle is $\pi\,\text{rad}$) which is tangent at the pericenter (or apocenter) of the parking (or target) orbit, see Fig. 4.

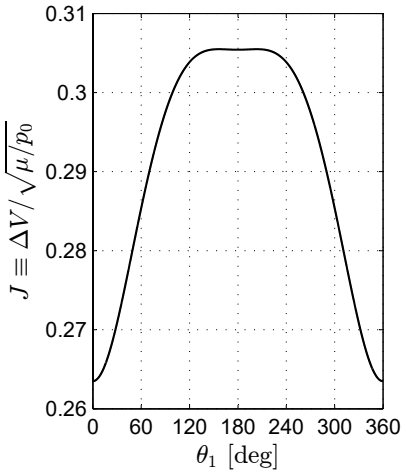

(a) Dimensionless ΔV.

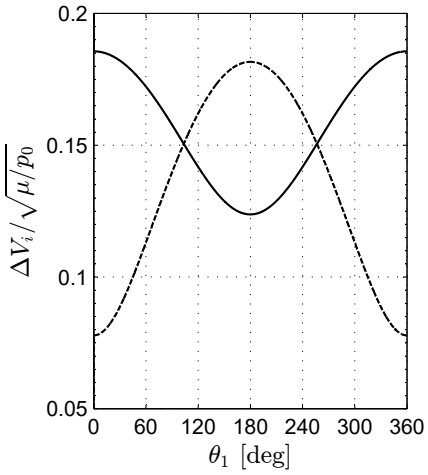

(b) Dimensionless ΔV_1 (solid line), and ΔV_2 (dashed line).

Figure 3: Dimensionless velocity variations as a function of θ_1 when $p_2/p_0 = 2$, $e_0 = 0.2$, $e_2 = 0.4$, and $\omega_2 = 0\,\text{deg}$.

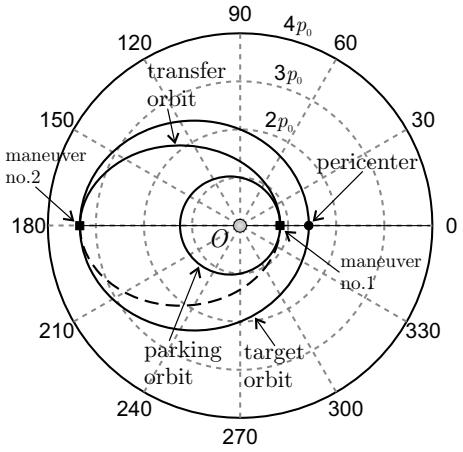

Figure 4: Parking, target, and optimal transfer orbits when $p_2/p_0 = 2$, $e_0 = 0.2$, $e_2 = 0.4$, and $\omega_2 0\,\text{deg}$.

This result is in perfect agreement with the conclusions of Lawden [22], who stated that "if two orbits have their axes aligned and the orbits either intersect or have their axes directed in the same sense, then the *over-all* optimal transfer orbit is that which is tangential to both terminals at an apse on each and which passes through the apse most distant from the center of attraction". Note that, in this case, the ratio of the primary body-apocenter distance of the target orbit to that of the parking orbit is about 2.66. Therefore, the apocenter of the target orbit is the apse most distant from the center of attraction, see Fig. 4.

When the value of ω_2 is different from zero (or 180 deg), the analysis of the optimal, cotangential, transfer trajectory is not so simple, but may be studied with the previous algorithm. For example, consider now $p_2/p_0 = 2$, $e_0 = 0.2$, $e_2 = 0.4$, and $\omega_2 = 60\,\text{deg}$ and assume $\theta_1 = 0\,\text{deg}$. From Eq. (37), it is found that $\Delta\theta \simeq 147.8\,\text{deg}$, where $a \simeq -0.3464$, $b = -1.2$, and $\psi \simeq -163.89\,\text{deg}$. This is a feasible value, since $f(\theta_1, \Delta\theta) > 0$, see also Fig. 5, where the function

$$G(\theta_1, \Delta\theta) \triangleq g(\theta_1, \Delta\theta) - e_2 \tag{39}$$

is drawn with $g(\theta_1, \Delta\theta)$ given by Eq. (31).

The solution corresponding to $\theta_1 = 0$ is $\theta_2 \simeq 147.8\,\text{deg}$, see Eq. (11), while $\eta_1 \simeq 1.1010$ from Eqs. (27)

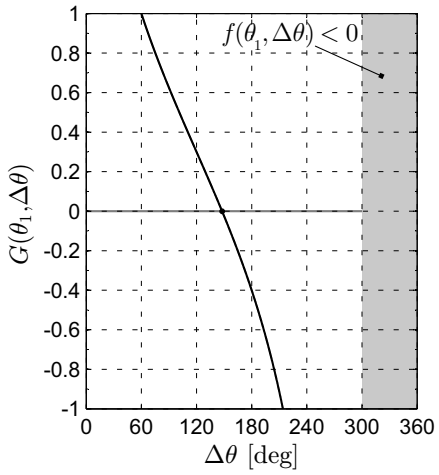

Figure 5: Function $G(\theta_1, \Delta\theta)$, see Eq. (39), when $\theta_1 = 0\,\text{deg}$, $p_2/p_0 = 2$, $e_0 = 0.2$, $e_2 = 0.4$, and $\omega_2 = 60\,\text{deg}$.

and (30) and $\eta_2 \simeq 1.2845$ from Eq. (28) and (30). Having calculated the four parameters $\{\eta_1, \eta_2, \theta_1, \theta_2\}$, the transfer orbit characteristics are $p_1/p_0 \simeq 1.2121$, see Eq. (12), $e_1 \simeq 0.4545$, see Eq. (13), and $\omega_1 = 0\,\text{deg}$, see Eq. (14). The dimensionless radial distance at the two maneuvers is $r_1/p_0 \simeq 0.8333$ from Eq. (17), and $r_2/p_0 \simeq 1.9698$ from Eq. (18). Finally, the velocity variations are $\Delta V_1/\sqrt{\mu/p_0} \simeq 0.1212$ from Eq. (21) and $\Delta V_2/\sqrt{\mu/p_0} \simeq 0.1709$ from Eq. (22), while the performance index is $J \equiv \Delta V/\sqrt{\mu/p_0} \simeq 0.2921$ from Eq. (23). The transfer trajectory is illustrated in Fig. 6, which shows its tangency with both the initial and the target orbit.

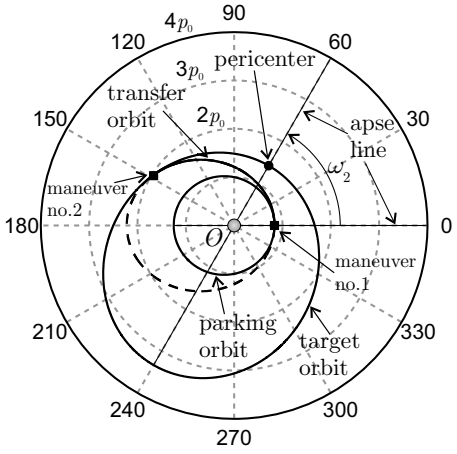

Figure 6: Parking, target, and transfer orbits when $\theta_1 = 0\,\text{deg}$, $p_2/p_0 = 2$, $e_0 = 0.2$, $e_2 = 0.4$, and $\omega_2 = 60\,\text{deg}$.

The dimensionless velocity variation $\Delta V/\sqrt{\mu/p_0}$ is easily calculated by varying the polar angle within the range $\theta_1 \in [0,\, 2\pi)$, see Fig. 7(a). Likewise, Fig. 7(b) shows the dimensionless functions $\Delta V_1 = \Delta V_1(\theta_1)$ and $\Delta V_2 = \Delta V_2(\theta_1)$, while $\{p_1,\, e_1,\, \omega_1\}$ and $\Delta\theta$ are reported in Fig. 8. The function $J = J(\theta_1)$ has a minimum (with $\min(J) \simeq 0.2776$) at a polar angle $\theta_1 = \theta_1^\star \simeq 82.4\,\text{deg}$, see Fig. 7(a), which corresponds to the optimal transfer. Using the previous method, it is found that $\theta_2 \simeq 223.07\,\text{deg}$, $\eta_1 \simeq 1.2016$, and $\eta_2 \simeq 1.1769$. The characteristics of the transfer orbit are $p_1/p_0 \simeq 1.4439$, $e_1 \simeq 0.5607$, and $\omega_1 \simeq 51.7\,\text{deg}$, the radial distances at maneuver points are $r_1/p_0 \simeq 0.9742$ and $r_2/p_0 \simeq 3.2398$, while the velocity variations are $\Delta V_1/\sqrt{\mu/p_0} \simeq 0.2108$, and $\Delta V_2/\sqrt{\mu/p_0} \simeq 0.0668$, see Fig. 7(b). The optimal transfer orbit, whose geometrical characteristics are much different from that corresponding to $\theta_1 = 0$, is illustrated in Fig. 9.

The joint use of Figs. 7 and 8 allows a tradeoff-analysis to be made between ΔV and the transfer

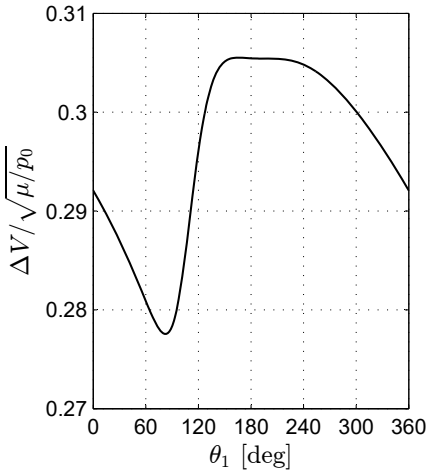

(a) Dimensionless ΔV.

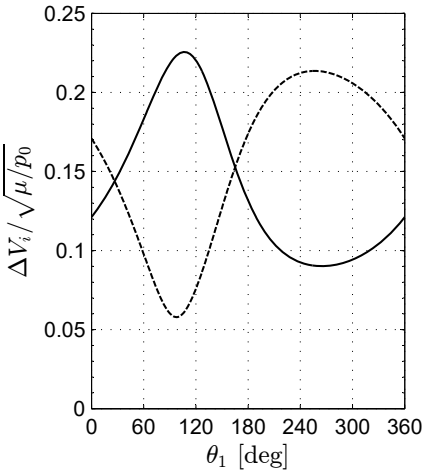

(b) Dimensionless ΔV_1 (solid line), and ΔV_2 (dashed line).

Figure 7: Dimensionless velocity variations as a function of θ_1 when $p_2/p_0 = 2$, $e_0 = 0.2$, $e_2 = 0.4$, and $\omega_2 = 60\,\text{deg}$.

orbit characteristics or the velocity variation at the two TIMs. Using again the same parking and target orbit as in the previous example, and assuming the maneuvers to be characterized by the same velocity variation, that is, $\Delta V_1 = \Delta V_2$, Fig. 7(b) shows that two different values of polar angle are possible, i.e. $\theta_1 \simeq \{26.6,\, 165.2\}\,\text{deg}$, with different total velocity variations $\Delta V_i/\sqrt{\mu/p_0} \simeq \{0.1438,\, 0.1527\}$, and distinct orbital parameters of the transfer orbit, see Fig. 10. As an additional example, it is also possible to look for the transfer orbit with the minimum eccentricity value. In fact, Fig. 8 shows that the minimum of the function $e_1 = e_1(\theta_1)$ is obtained at $\theta_1 \simeq 186.83$, when the eccentricity is $e_1 \simeq 0.0745$, and the total velocity variation is $\Delta V/\sqrt{\mu/p_0} = 0.3054$. The corresponding transfer trajectory is drawn in Fig. 11.

The last case study is consistent with that of the two satellites of the Galileo family named Doresa and Milena (that is satellite 5 and 6 of Galileo constellation). Due to a malfunction of the Soyuz Fregat launch vehicle, satellites Doresa and Milena were inserted into incorrect, highly elliptical orbits with semimajor axis 26192 km and eccentricity 0.2330 [23], later partially corrected to a value of 27977 km and about 0.15, respectively (more precisely, the eccentricity is 0.156 for satellite 5, and 0.15167 for satellite 6). Accordingly, assume $p_2/p_0 = 1.1019$, $e_0 = 0.233$, $e_2 = 0.1561$, and $\omega_2 = 0\,\text{deg}$. In this case, the proposed procedure gives an optimal (dimensionless) velocity variation of about $\Delta V/\sqrt{\mu/p_0} \simeq 0.0382$ with an initial polar angle equal to $\theta_1 = 0\,\text{deg}$.

4. Conclusions

In this paper, the classical problem of two-impulse optimal cotangential transfer between two coplanar elliptic orbits has been analyzed. Starting from a mathematical model that describes the spacecraft in a general multiple-impulse scenario, the transfer orbit characteristics, in terms of eccentricity, semilatus rectum, and apse line direction are obtained as a function of the angular position of the first tangential maneuver. The minimum velocity variation required to complete the two-dimensional transfer is the output of a semi-analytical method. A tradeoff-study that involves the mission performance index, the velocity variation of each maneuver, and the characteristics of the transfer orbit, may be easily completed with the aid of a set of graphs and compact analytical relations.

The proposed approach is useful for simplifying the analysis of complex mission scenarios that involve, for instance, three (or more) tangential, impulsive, maneuvers. In that case, however, the number of free mission parameters increases and the performance index becomes a function of multiple variables, so that a suitable numerical algorithm is required for obtaining the minimum value of the total velocity variation.

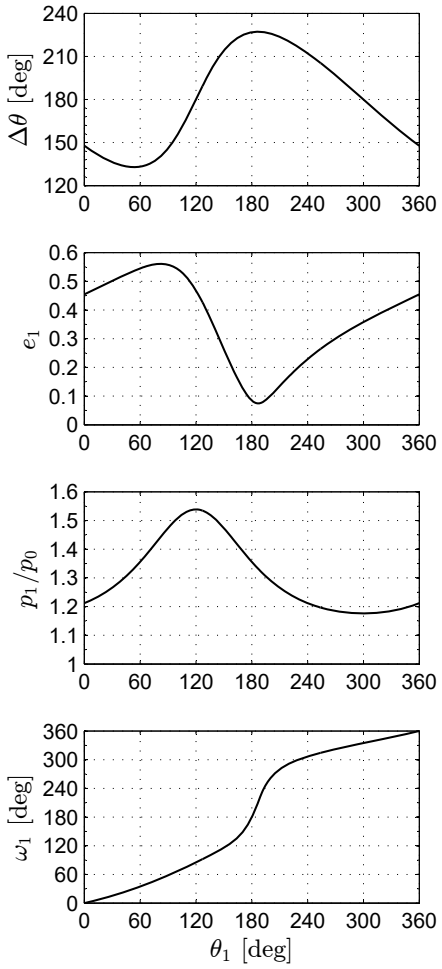

Figure 8: Spacecraft swept angle and transfer orbit characteristics as a function of θ_1 when $p_2/p_0 = 2$, $e_0 = 0.2$, $e_2 = 0.4$, and $\omega_2 = 60\,\mathrm{deg}$.

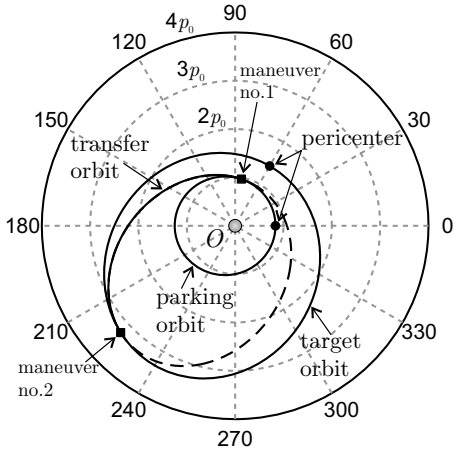

Figure 9: Optimal transfer orbit when $p_2/p_0 = 2$, $e_0 = 0.2$, $e_2 = 0.4$, and $\omega_2 = 60\,\mathrm{deg}$.

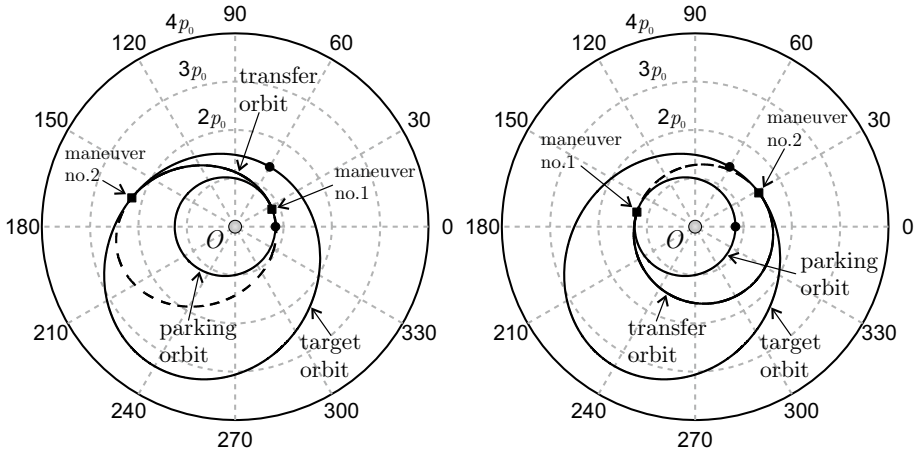

(a) $\theta_1 = 26.6\,\text{deg}$ and $\Delta V_i = 0.1438\sqrt{\mu/p_0}$. (b) $\theta_1 = 165.2\,\text{deg}$ and $\Delta V_i = 0.1527\sqrt{\mu/p_0}$.

Figure 10: Transfer with equal ΔV_i when $p_2/p_0 = 2$, $e_0 = 0.2$, $e_2 = 0.4$, and $\omega_2 = 60\,\text{deg}$.

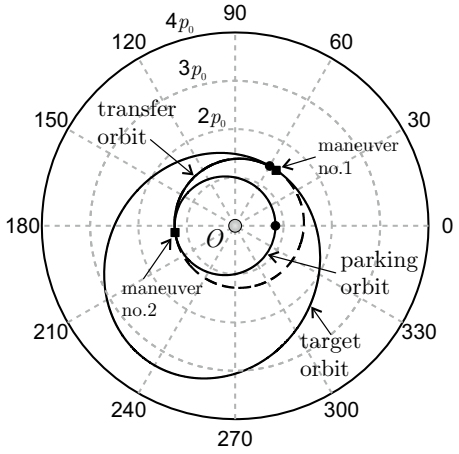

Figure 11: Transfer orbit with of minimum eccentricity when $p_2/p_0 = 2$, $e_0 = 0.2$, $e_2 = 0.4$, and $\omega_2 = 60\,\text{deg}$.

References

[1] H. D. Curtis, Orbital Mechanics for Engineering Students, 3rd Edition, Aerospace Engineering, Butterworth-Heinemann, 2013, Ch. 6, pp. 299–344, ISBN: 9780080977478.

[2] F. W. Gobetz, J. R. Doll, A survey of impulsive trajectories., AIAA Journal 7 (5) (1969) 801–834, doi: 10.2514/3.5231.

[3] D. F. Lawden, Orbital transfer via tangential ellipses, Journal of the British Interplanetary Society 2 (6) (1952) 278–289 .

[4] R. H. Battin, An Introduction to the Mathematics and Methods of Astrodynamics, Revised Edition, AIAA Education Series, American Institute of Aeronautics and Astronautics, Inc., Reston, VA, 1999, pp. 514–536, ISBN: 1-56347-342-9.

[5] B. Thompson, K. Choi, S. Piggott, S. Beaver, Orbital targeting based on hodograph theory for improved rendezvous safety, Journal of Guidance, Control, and Dynamics 33 (5) (2010) 1566–1576, doi: 10.2514/1.47858.

[6] Y. Meng, Q. Chen, Q. Ni, A new geometric guidance approach to spacecraft near-distance rendezvous problem, Acta Astronautica 129 (2016) 374–383, doi: 10.1016/j.actaastro.2016.09.032.

[7] G. Zhang, D. Zhou, D. Mortari, T. A. Henderson, Analytical study of tangent orbit and conditions for its solution existence, Journal of Guidance, Control, and Dynamics 35 (1) (2012) 186–194, doi: 10.2514/1.53396.

[8] G. Zhang, X. Cao, G. Ma, Reachable domain of spacecraft with a single tangent impulse considering trajectory safety, Acta Astronautica 91 (2013) 228–236, doi: 10.1016/j.actaastro.2013.06.016.

[9] N. X. Vinh, E. G. Gilbert, R. M. Howe, D. Sheu, P. Lu, Reachable domain for interception at hyperbolic speeds, Acta Astronautica 35 (1) (1995) 1–8, doi: 10.1016/0094-5765(94)00132-6.

[10] L. Xuehua, H. Xingsuo, Z. Qinfang, S. Ming, Reachable domain for satellite with two kinds of thrust, Acta Astronautica 68 (11-12) (2011) 1860–1864, doi: 10.1016/j.actaastro.2011.01.004.

[11] Q. Chen, D. Qiao, H. Shang, X. Liu, A new method for solving reachable domain of spacecraft with a single impulse, Acta Astronautica 145 (2018) 153–164, doi: 10.1016/j.actaastro.2018.01.040.
[12] R. E. Burns, Forbidden tangential orbit transfers between intersecting Keplerian orbits, Acta Astronautica 19 (8) (1989) 649–556, doi: 10.1016/0094-5765(89)90133-1.
[13] E. V. Kiriliuk, S. A. Zaborsky, Optimal bi-elliptic transfer between two generic coplanar elliptical orbits, Acta Astronautica 139 (2017) 321–324, doi: 10.1016/j.actaastro.2017.07.006.
[14] L. Iorio, Editorial for the special issue 100 years of chronogeometrodynamics: The status of the Einstein's theory of gravitation in its centennial year, Universe 1 (1) (2015) 38–81, doi: 10.3390/universe1010038.
[15] I. Debono, G. F. Smoot, General relativity and cosmology: Unsolved questions and future directions, Universe 2 (4) (2016) 23/1–23/82, doi: 10.3390/universe2040023.
[16] W. L. Wen, A study of cotangential, elliptical transfer orbits in space flight, Journal of the Aerospace Sciences 28 (5) (1961) 411–417, doi: 10.2514/8.9010.
[17] G. Zhang, D. Zhou, Z. Sun, X. Cao, Optimal two-impulse cotangent rendezvous between coplanar elliptical orbits, Journal of Guidance, Control, and Dynamics 36 (3) (2013) 677–685, doi: 10.2514/1.59191.
[18] N. X. Vinh, A property of cotangential elliptical transfer orbits, AIAA Journal 2 (10) (1964) 1841–1844, doi: 10.2514/3.2686.
[19] H. G. Moyer, An analytic treatment of cotangential transfer, AIAA Journal 5 (6) (1967) 1197–1198, doi: 10.2514/3.4164.
[20] J. Whiting, Orbital transfer trajectory optimization, Master's thesis, Massachusetts Institute of Technology (February 2004).
[21] A. A. Quarta, G. Mengali, Linear systems approach to multiple-impulse trajectory analysis via regularization, Journal of Guidance, Control, and Dynamics 33 (5) (2010) 1679–1683, doi: 10.2514/1.50133.
[22] D. F. Lawden, Optimization Techniques - With Applications to Aerospace Systems, Vol. 5 of Mathematics in Science and Engineering, Academic Press, New York, 1962, Ch. 11, pp. 323–351, ISBN: 978-0-12-442950-5.
[23] J. Paziewski, R. Sieradzki, P. Wielgosz, On the applicability of Galileo FOC satellites with incorrect highly eccentric orbits: An evaluation of instantaneous medium-range positioning, Remote Sensing 10 (2) (2018) 208/1–208/19, doi: 10.3390/rs10020208.